Rimantas Barauskas,
***Julija Baltušnikaitė,**
***Aušra Abraitienė,**
***Diana Grinevičiūtė**

Department of System Analysis,
Kaunas University of Technology,
Studentu 50, LT – 51368 Kaunas, Lithuania.
E-mail: rimantas.barauskas@ktu.lt

***SRI Center for Physical Sciences and Technology,**
Textile Institute,
Demokratu 53, LT – 48485 Kaunas, Lithuania.

Experimental Investigations and Finite Element Model of Heat and Moisture Transfer in Multilayer Textile Packages

Abstract
New textile technologies based on lamination and thermoplastic film or volumetric textile architecture creation enable to achieve many desirable effects providing necessary ballistic protection along with a considerable improvement in wearing comfort. In this study a prototype active ventilation system of a 3D textile layer was developed and investigated. The finite element, which represents the forced ventilation layer made of three-dimensional textile material, was created and may be used as a structural element within the overall structural model of the textile package. The element equations are derived on the basis of an ideal gas state equation. Results of the textile layer characteristics measured and numerical data are presented.

Key words: *textile multi-layers, ventilation, thermal transport, moisture transport, finite element modeling.*

Introduction

Multi-layer textile packages (MTP) are widely used for protection against ballistic impacts and the influences of dangerous environments [1, 2]. One of the important challenges for ballistic protection clothing designers is to ensure wearing comfort by providing the necessary thermal and moisture concentration balance at the human skin surface.

In modern protective clothing manufacturing a number of fabrics of different structure and composition (woven, nonwoven, knitted, multilayer, etc.) are used. Such fabrics can be processed with different surface treatments or finishing technologies and have very different characteristics of wearing comfort. It is important to note that for evaluation of such materials different investigation methods are applied. New materials designated for the development of protective clothing usually enter the manufacturing process still not investigated properly or the results of such investigations are obtained using different methods. For this reason it is rather difficult to predict and describe theoretically the heat and moisture processes in multilayer protective clothing [3 – 7].

Theoretical investigations of wearing comfort characteristics of new generation textiles are complicated because of the heterogeneous internal structure, coupled heat and moisture transfer and other physical processes, which occur in different space and time scales. During the last decade numerous researches have been carried out regarding the mathematical modeling of different aspects of the physical behaviour of fabric structures. The models described in [8] analysed the simultaneous heat and moisture transfer in porous textiles with phase change materials (PCM). A model of micro-PCM was introduced and a patch of textiles was treated as a continuum model by using the finite volume method. Paper [9] investigated the phenomena of condensation in three-layer waterproof breathable fabrics for clothing. Water vapour transfer as condensation occuring within the three-layer waterproof breathable fabrics was based on the simultaneous heat and mass transfer theory.

Models considering natural ventilation in clothes were formulated in [10 – 12]. Clothing contact with the human body is presented by means of two non-concentric cylinder systems, where the internal one can move, imitating microclimate gap change in the wearing conditions of walking humans. The equations describe the motion of air and water vapour within the gap simultaneously with the heat transfer by means of conduction and convection. A description was also given of the means by which the fabric and fabric-to-skin macroscopic heat and mass transfer internal transport coefficients could be determined.

Equations of thermal conduction and moisture diffusion in a unit cell of a fibrous material, as well as in a unit cell of a woven fabric were formulated in [13]. By applying the homogenisation method, the equations were extended to be applied to finite size domains of the fabric. A mathematical model which considers the woven fabric as a system of porous yarns, interlacements between warp and weft yarns and air pores as well as all the basic weaves in order to predict the thermal resistance of the fabric is presented in paper [14]. The conduction and radiation heat transfer together was calculated based on the construction parameters of the fabric. The thermal insulation, which is equivalent to the thermal resistance, was predicted with the help of these parameters. Modern textile technology provides many unique solutions for satisfying the requirements of the fibrous material configuration, construction and properties. The capability of creating volumetric (3D) textile architectures aroused tremendous interest for advanced technical applications in the aerospace and automotive industries [15, 16].

To ensure an optimum body climate and protect the wearer against possible thermal shock under extreme conditions when wearing modern ballistic protection equipment, it is necessary to eliminate excess body heat. A number of systems reducing the thermal barrier between the protective clothing and the human body, ensuring an optimal microclimate, are being developed in the world. Depending on the technical solutions and cooling methods, these systems are divided into two types: passive and active cooling systems. The most unsophisticated passive cooling system which could ensure satisfactory microclimate conditions is the cooling of the human body by inserting an additional layer of porous material or 3D textiles between the body and clothing. The other techniques of passive cooling systems are based on the usage of PCM [17, 18] or shape memory polymers [19], as well as on the principle of evaporation cooling [20].

Barauskas R, Baltušnikaitė J, Abraitienė A, Grinevičiūtė D. Experimental Investigations and Finite Element Model of Heat and Moisture Transfer in Multilayer Textile Packages.
FIBRES & TEXTILES in Eastern Europe 2012; 20, 6A(95): 112-118.

Passive body cooling systems are effective only for a short time and during low physical activity. For active cooling systems the forced flow of cold liquid, usually water or a water-glycol mixture, is used [21]. The principle of the air ventilation system is based on permanent air movement in the vicinity of the human skin by using a tube system or cooling zones formed by appropriate separators and elimination of heat excess through clothing openings (collar, armpits, torso opening). Different methods of air ventilation may be applied, as well as different systems which may be stationary or mobile [22].

This work presents a new structural model for computational modelling of the heat and water vapour exchange process through composite textile multi-layers. Equations are formulated for an element which represents a single textile layer with nodes situated in the inter-layer air gaps. The equations of elements are related to the structural equation in accordance with the standard discrete system approach [23]. Air and water vapour mass and heat transport as well as convective heat exchange through the layers of the textile package are described by using appropriate water vapour transmission and heat conduction coefficients as physical constants. A heat and water vapour exchange model of the forced ventilation layer made of 3D textiles is described [24]. A prototype active ventilation system of the 3D textile layer was developed and experimented with.

Experimental

Development and investigation of a cooling system of controlled intensity integrated into a bullet-proof vest

The model proposed is based on the air ventilation principle (active cooling). In order to achieve a more sensible effect, extra cooling is provided by a thermoelectric (Peltier) module (passive cooling), which decreases the environmental temperature and provides cool air into the ventilation system. The principal scheme of the cooler system is presented in ***Figure 1***. The cooling system is integrated into a bullet-proof vest. Cooling is supplied to the area of the waist and chest, while excess heat is eliminated through the neck and armpit areas. To create an air circulation layer, 7.5 mm thick knitted fabric of 100% PES was used. The inner layer of the spacer material is resistant to compression and therefore could successfully be used as an air-gap. The system of perforated rubber tubes was integrated into 3D material in order to distribute the incoming air over the cooled surface. ***Figure 2*** presents an inside view of the bullet-proof vest with integrated tube system. The air flow of the system was created by a rotary air blower, with a power of 24 W and air flow of 460 l/min, ***Table 1***. The system enabled automatic cooling process monitoring by means of the incorporated programmable device with data processing and compiler system and thermocouples measuring the temperature. For operation of the system a power supply unit of 12 V DC was used. For extra cooling of the environment air a thermoelectric Peltier module was integrated.

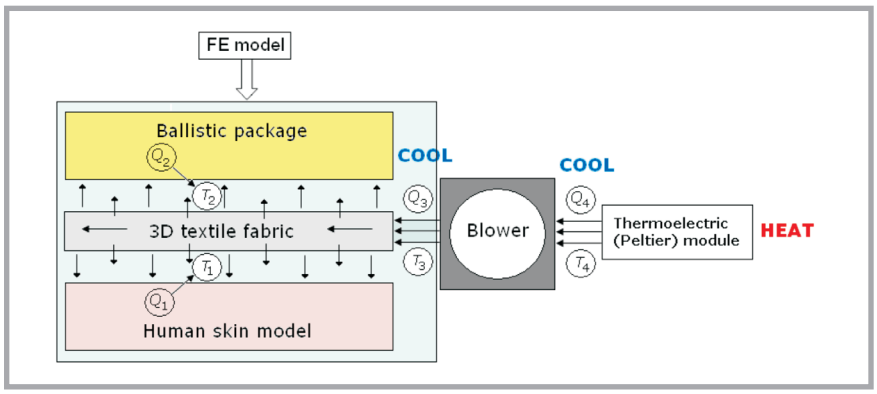

Figure 1. *Principal scheme of heat and moisture exchange in the active cooler system.*

Table 1. *Technical parameters of the rotory air blower.*

View of the blower	Characteristic	U150 R	U150R
	Nominal voltage, V	12	24
	Operating voltage, V	6 - 13.5	12 - 27
	Nominal amperage, mA	2330	2380
	Operating amperage, mA	2030	2050
	Power, W	24	49
	Rev number, min^{-1}	8850	11600
	Air flow, l/min	460	560
	Pressure, Pa	1390	2420
	Mass, kg	0,340	0,340
	Operating temperature, ºC	-20 … +65	-20 … +65
	Overall dimensions, mm	143.5×135.7×47.5	143.5×135.7×47.5

Results and discussion

Experimental investigation of the cooling efficiency of the system was carried out. For simulation of the heat power released by the human skin surface we used an adjustable heater, which was able to maintain the surface temperature at approximately 37 ºC. For measuring the temperature between the ballistic package and heated surface, thermocouples were applied. Thermal views of the cooling effect created by the system were fixed by employing a thermovisor.

Optimum microclimate conditions were supported by the temperature control system, which was designed to automatically activate cooling as the body temperature rises to the predefined upper limit. After cooling the body to a comfort temperature (lower limit) a thermostat turned off the cooling system. In this way, the human body is protected from overheating and cold, and battery power is also saved.

In this case the thermostat was programmed to reach 37 °C temperature, at which the blower was activated and the

Figure 2. *Inside view of the ballistic vest with integrated cooling system.*

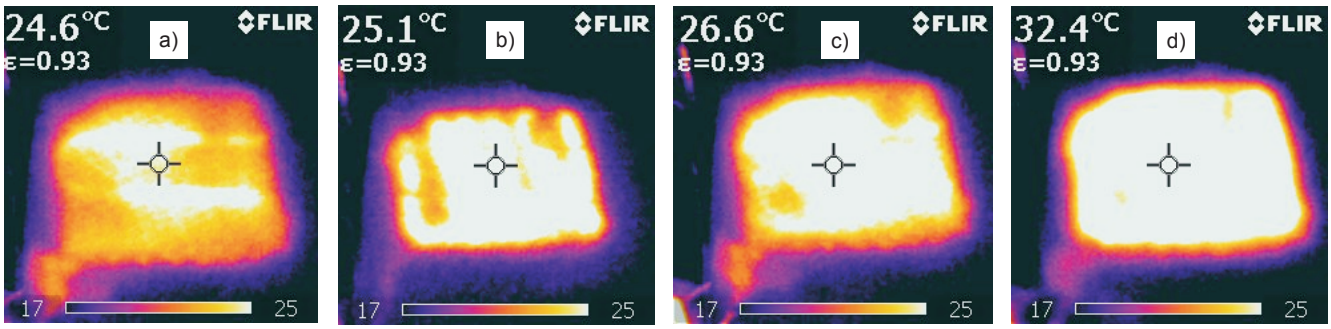

Figure 3. *Thermal picture of the inner side of the ballistic vest after operation of the cooling system for 2 min (a), 6 min (b), 10 min (c), and after the shut down of the cooling system (d).*

Peltier thermocouple started operating. The Peltier thermocouple was mounted in such a way that the cold side with an additional cooling radiator supplied cold air directly into the exit hole of the blower. The ventilator blew air through a system of tubes into 3D textile material, which allowed the air to distribute uniformly over the cooled surface. Experimental results are presented in thermal images, ***Figure 3***.

Computational model

In parallel with the empirical approach and innovative design, attempts to theoretically investigate and explain the heat and water vapour exchange phenomena in the textile multi-layers have been made. The physical processes of heat and water vapour exchange on multi-layer textiles are very complex. It is hard to obtain reliable quantitative results regarding the temperatures and amount of sweat established in the micro-climate gap in real wearing conditions. Nevertheless the basic phenomena can be modelled and simulated using computational models. By regarding the length scale of the model at the level of the thickness of an individual textile layer, a discrete structural model can be built in order to present the average temperatures and amounts of water vapour at each layer as they change in time.

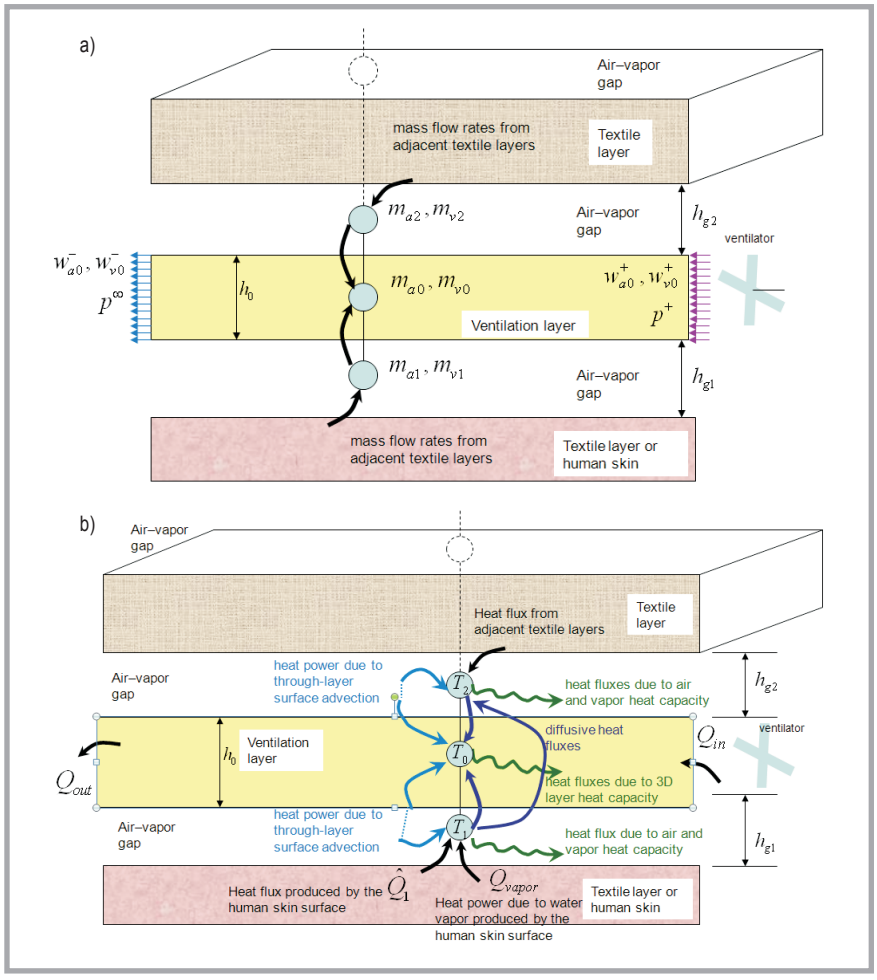

Figure 4. *Flow rates of air and water vapour (a) and heat fluxes (b) in the r finite element of the ventilation laye.*

In this study the finite element approach has been employed. A new structural element has been developed which is suitable to present the time law of temperature and water vapour concentration change within the 3D textile-based ventilation layer and in-between of the layers. As input parameters, the heat power and water vapour generated at the surface of human skin, the environment temperature as well as the flow rate, temperature and humidity of incoming air are used.

The basic relations of the flow rate and heat balance equations of finite elements of textile layers were derived in our publication [24]. As a prototype structure which incorporates the idea of the finite element of the ventilation layer , the scheme presented in ***Figure 4*** should be regarded. The ventilation layer is situated in-between the human body and textile package. The forced air flow created by means of a ventilator is supplied to the inlet of the ventilation layer.

In our model the finite element of the ventilation layer is formulated as follows: The finite element of the ventilation layer has three nodes, two of which (nodes 1 and 2) are situated in the gaps at the bottom and top of the 3D layer correspondingly, and the third node (node 0) represents the inside of the ventilation layer, ***Figure 4***. Very often node 1 coin-

cides with the surface of the human skin. We assume that the overall heat and mass exchange mechanism in the textile multilayer consists of several physical processes, which take part simultaneously. The temperatures, as well as the air and water vapour partial pressures in the gaps at the top, bottom and inside of the ventilation layer may have different values. Therefore the gas (water vapour and air mixture) may penetrate through the layer, as well as some quantity of water vapour may be accumulated therein. Heat is transferred by convection because of gas penetration through the openings of the layer and by heat conduction through the solid parts of the honeycomb-like structure of the layer.

The nodal variables of the finite element are masses m_{v1}, m_{v2}, m_{v0} of water vapour and masses m_{a1}, m_{a2}, m_{a0} of air contained in the inter-layer gaps and within the ventilation layer, as well as temperatures T_1, T_2, T_0 in the inter-layer gaps and in the ventilation layer. The geometry of the element is described by sizes h_{g1}, h_{g2} of the gaps, the ventilation layer thickness h_0 and area A, ***Figure 4***.

The finite element equations are derived by using the principle of balance of incoming and outgoing flow rates and heat fluxes at each node as ***Equations 9 - 11*** where:

c_v, c_a - specific (mass) heat capacity coefficients of water vapour and air;

$\tilde{w}_{v1}, \tilde{w}_{a1}, \tilde{w}_{v2}, \tilde{w}_{a2}$ are the flow rates of water vapour and air through the bottom and top surfaces of the 3D ventilation layer to the gaps at both sides of the layer;

w_{a1}, w_{v1}, w_{a2}, w_{v2}, are the flow rates of water vapour and air transferred to the gaps from adjacent textile layers or from the human skin;

w^{+}_{a0}, w^{+}_{v0} are the flow rates of water vapour and air supplied to the inlet of the ventilation layer by the ventilator;

Q_{in}, Q_{out} are the heat powers due the mass flow rates through the inlet and outlet of the ventilation layer;

$\hat{\tilde{w}}_{v1}$ is the mass flow rate of water vapour generated by the human skin;

p^{+} in Pa - full pressure at the inlet created by the ventilator;

T_{∞} is the air temperature of the external environment;

T_{human} is the air temperature at the surface of the human skin;

$\hat{Q}_1$, Q_{vapor} are heat powers produced by the human skin and contained in water vapour produced by the human skin correspondingly;

$Q_{adv}01$, $Q_{adv}10$ are the convection heat fluxes at the two sides of the bottom surface of the ventilation layer;

$Q_{adv}02$, $Q_{adv}20$ are the convection heat fluxes at both sides of the top surface of the ventilation layer;

$Q_{diff}10$, $Q_{diff}20$, $Q_{diff}12$ are the diffusive heat fluxes between pairs of nodes 1-0, 2-0 and 1-2 of the element due to heat conduction through the solid structure of the 3D textile layer;

Q_2 is the heat flux from the adjacent textile layer.

$$\begin{cases} \tilde{w}_{v1} + \tilde{w}_{v2} + w^{+}_{v0} - w^{-}_{v0} - \dot{m}_{v0} = 0; \\ \tilde{w}_{a1} + \tilde{w}_{a2} + w^{+}_{a0} - w^{-}_{a0} - \dot{m}_{a0} = 0; \\ Q_{diff\,10} + Q_{diff\,20} + Q_{adv10} + Q_{adv20} - \left(c_a m_{a0} + c_v m_{v0}\right)\dot{T}_0 + Q_{in} - Q_{out} = 0; \end{cases} \quad (9)$$

at the central node,

$$\begin{cases} w_{v1} - \tilde{w}_{v1} - \dot{m}_{v1} = 0; \\ w_{a1} - \tilde{w}_{a1} - \dot{m}_{a1} = 0; \\ \hat{Q}_{\text{üüüü}} + c_v \hat{\tilde{w}}_v T_{human} - \left(c_a m_a + c_v m_v\right)\dot{T} - Q_{diff} - Q_{diff} + Q_{adv} = 0 \end{cases} \quad (10)$$

at the bottom node and

$$\begin{cases} w_{v2} - \tilde{w}_{v2} - \dot{m}_{v2} = 0; \\ w_{a2} - \tilde{w}_{a2} - \dot{m}_{a2} = 0; \\ Q_2 - \left(c_a m_{a2} + c_v m_{v2}\right)\dot{T}_2 - Q_{diff\,20} + Q_{diff\,12} + Q_{adv20} = 0 \end{cases} \quad (11)$$

at the top node of the finite element,

Equations 9, 10, and 11.

The variables presented in ***Equations 9 - 11*** are related by employing the ideal gas state equation, the heat conductivity relations and the relation of heat transfer due to the mass flow rates of water vapour and air. The final equation system of the finite element with the left-hand side capacity matrix of dimension 9 × 9 may be represented in an abbreviated form as

$$\left[\mathbf{C}\left(\{\mathbf{U}\}\right)\right]\{\dot{\mathbf{U}}\} = \left\{\mathbf{Q}\left(\{\mathbf{U}\}, w^{+}_{v0}, w^{+}_{a0}, p^{+}, T_{\infty}, p^{+}, T_{\infty}, \hat{\tilde{w}}_{v1}, \hat{Q}_1, Q_{vapor}\right)\right\}; \quad (12)$$

where: $\{\mathbf{U}\} = \{m_{v0} \quad m_{a0} \quad T_0 \quad m_{v1} \quad m_{a1} \quad T_1 \quad m_{v2} \quad m_{a2} \quad T_2\}$ - is the vector of nodal variables of the finite element.

The equation obtained (12) is of the highly non-linear differential type. The element equations are related to the structural differential equation, which is solved by using computational routines designed for solving stiff differential equations.

The finite element of the 3D ventilation layer derivedis a powerful analysis tool, by means of which the heat and water vapour exchange in textile packages can be investigated. It may be used in combination with the finite element of the textile layer, the equations of which also have been published by us in [24]. The model based on the finite elements developed may adequately represent any array of different layers in a complex textile multi-layer and to simulate the change in temperature and water vapour concentration within all inter-layer gaps in time.

Two inherent restrictions of the elements derived need to be pointed out. First each element presents the whole textile layer and is not able to present the non-uniformity of air flow over the surface thereof. Secondly the simulation is correct up to the point when sweating takes place, as the model is mathematically based on the ideal gas state equation.

Numerical results

The finite element model developed has been implemented by us and can be run in MATLAB or Octave mathematical software environments. The practical need to analyse packages made of modern textile materials encounters difficulties because of unknown physical parameter values, such as heat transfer, heat ca-

Table 2. Characteristics of the textile materials

Material	Area density, g/m²	Thickness, mm	Water vapour transmission coefficient δ_p, m²Pa/W=s/m	Water vapour resistance R_{et}, m²Pa/W	Air permeability ψ_a, mm/s	Air mass permeability coefficient k_a, s/m	Thermal resistance R_t, m²/W	Heat transfer coefficient α_t, W/m² K
Twaron LFT GF4	5300	6.0	0	0	0	0	0.183	5.46
Twaron CT709	6400	9.6	0	0	0	0	0.124	8.06
Dyneema	5300	7.3	0	0	0		0.132	7.56
3D textile	520	7.5	3.4589×10^{-5}	6.36	404	0.00475	0.118	8.47

pacity, water vapour transmission and air permeability coefficients, water vapour capacity and others used in the model developed. Many parameters can be measured by using appropriate standard procedures, such as [25] for determining water vapour resistance R_{et}, m² Pa/W and thermal resistance θ, m² K/W, and [26] for determining the air permeability coefficient ψ_a, mm/s.

Some experimental measurement results of materials are provided in ***Table 2***. Values of unknown heat and hydraulic capacity parameters are difficult to measure, approximate values of which have been calculated on the basis of the values presented in [27] and then adjusted more finely by comparing the numerical simulation results against those of certain physical experiments. We hope that even with rough estimations of capacity parameter values, errors in the modelling results are not crucial as they may influence only the duration of complex interaction processes rather than the state of thermal and water vapour concentration equilibrium obtained. On the other hand, the innovative solutions of smart textiles provide wide spectra of materials with different physical properties, therefore theoretical analysis of the influence of the parameters on wearing comfort conditions are of considerable value.

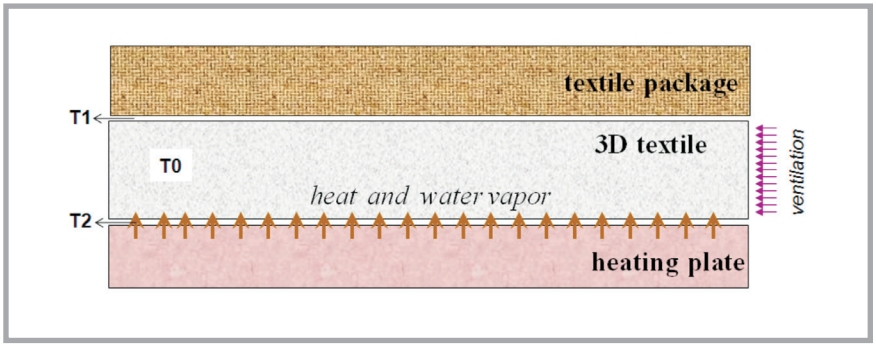

Figure 5. *Experimental scheme of measurement of heat convection by means of forced ventilation.*

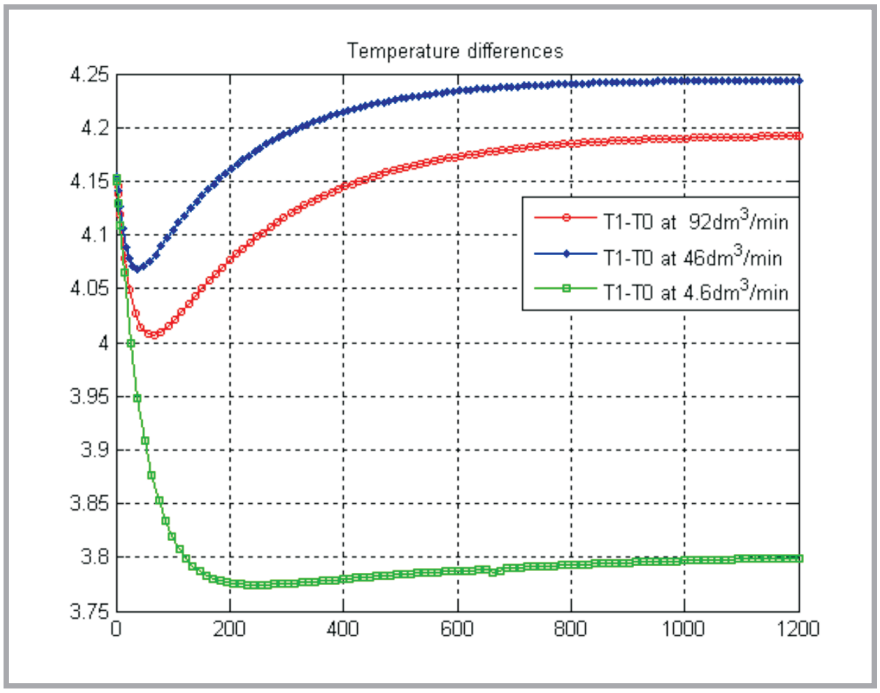

Figure 6. *Differences in air temperatures in microclimate gap and ventilation layer at three different ventilation rates; heating power 25 W, outer surface covered by Twaron CT709 textile package, outer(ventilation) temperature 291 K. Material constants α_{3D} = 4.95 W/(m²K), $\tilde{\alpha}_{3D}$ = 20 W/(m²K), α_{3D} = 1800 J/(m²K), $\alpha_{package}$ = 8.06 W/(m²K), area 0.24 m².*

Analysis of temperatures in the ventilation layer covered by the textile package. Pure heating.

The calculations demonstrate the process of heat convection from the ventilation layer by the ventilation air flow, ***Figure 5***.

As the side boundaries of the ventilation layer can be treated as a free outlet, the model assumes a constant pressure value within the layer, which is equal to the environment pressure. Conversely the gaps between each layer of textiles as well as between the textiles and heating plate (human skin) are assumed to be isolated from the environment at their side boundaries. Therefore the pressure within the gaps can increase due to an increase in the temperature. Heat and mass exchange can take place only through the top and bottom of each gap because of the permeability of the neighbouring textile surfaces to air, water vapour and heat. The value of the heat transfer coefficient of the ventilation layer α_{3D} = 8.4746 W/(m² K) is based on measurements in accordance with standard [20], ***Table 2***. In reality, experimental values of constants of the ventilation layer correspond to the combined permeability of the 3D honeycomb-like structure itself and of the air, which is always present within the ventilation layer. We used $\tilde{\alpha}_{3D}$ = 20 W/(m² K) as a close-to-reality value, which produced reasonable results, as shown when experimentally measured temperatures inside and outside of the ventilation layer were com-

pared with each other. The heat capacity value c_{3D} = 1800 J/(m^3 K) is also selected in order to obtain the time law of temperature increase close to the experimental. On the other hand, the heat capacity value does not influence the final temperature value when the state of thermal equilibrium is reached. Permeability coefficients of the top and bottom surface of the ventilation layer to water vapour and air are δ_p = 3.4589×10^{-3} m^{2}Pa/W; k_a = 0.075 m^{2}Pa/W.

The time laws of the air temperature in the ventilation layer (T_0), in the gap at the textile package Twaron CT709 (T_1) and at the heating plate (T_2) have been calculated at given different ventilation rates v^+ = 4.6 dm^3/min, v^+ = 46 dm^3/min, and v^+ = 92 dm^3/min, ***Figure 6***. Notice that even at very low rates of ventilation air flow the temperature difference T_1 - T_0 does not converge to zero because of different pressures in the ventilation layer and microclima gap and because of heat exchange, which takes place through the side opening of the ventilation layer to the outer environment.

It is not easy to ensure reliable temperature measurements in inter-layer gaps for comparison between computed and experimental results. An attempt at validation of the results computed has been made in this study, the results of which are presented in ***Figure 7***. Despite the quite large dispersal of experimental points, the overall quantitative and qualitative similarity of the results computed to those of the experiment can be noticed. It should be mentioned that the measurements were performed by inserting a thin thermometer into the ventilation layer close to the input of the air tube, therefore certain deflections of the temperatures measured from the average value over the layer were inevitable.

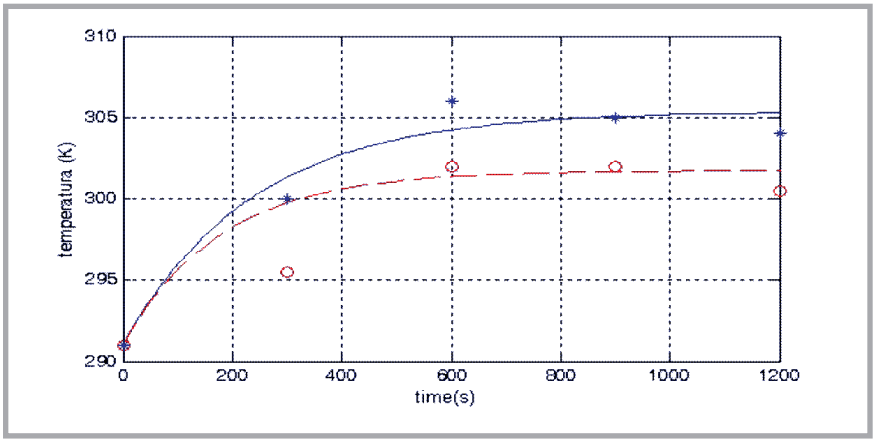

Figure 7. *Comparisson of computed and experimental temperatures T0 time laws within the 3D ventilation layer. Heating 20 W, ——, * - no ventilation airflow, - - - -, o - ventilation 23 dm^3·min^{-1}.*

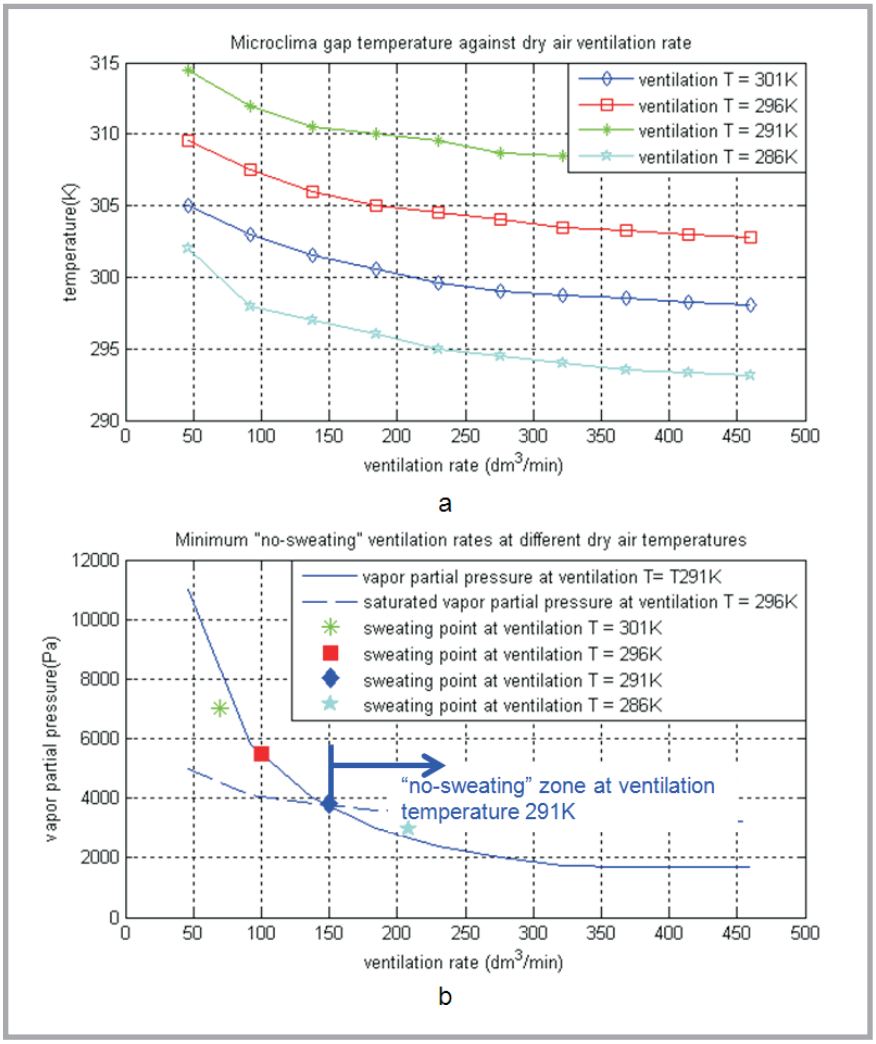

Figure 8. *Equilibrium temperatures (a) and water vapour partial pressures (b) in the microclimate gap in relation to the ventilation rate at different values of ventilation air flow temperatures.*

Calculating ventilation rates and predicting sweating situations

As the model can be used to obtain the water vapour partial pressures and temperatures in inter-layer gaps, the sweating situations can be predicted. The sweating conditions take place as the partial pressure of the water vapour in the microclima gap is equal to the saturated water vapour pressure at the temperature obtained in the microclima gap. ***Figure 8*** presents the dependencies of equilibrium temperature and water vapour partial pressure in the microclimate gap on the ventilation rate. Absolutely dry air (no vapor) ventilation is assumed. Intersection of the water vapour partial pressure and the saturated vapour pressure curves in ***Figure 8.b*** provides the minimum value of the ventilation rate, below which steady sweating takes place. The bold markers identify the minimum ventilation rates and the corresponding partial water vapour pressure values under which steady

sweating begins. Each marker corresponds to the individual ventilation air temperature prescribed, indicated in ***Figure 8***. This enables to determine ventilation rates which ensure no-sweating and temperature comfort conditions.

Conclusions

A new experimental ventilation system of the ballistic protection jacket was introduced in this work. A simulation model of a warrior ballistic protection clothing micro-climate system has been developed. It was demonstrated that the optimum result may be achieved by combining the passive and active cooling systems. The integration of a 3D textile-based ventilation layer in between the ballistic protection textile package and human body enabled to create a controlled cooling system, where the temperature of air at the inlet is regulated by a thermoelectric module. The sweat and excess heat are removed by means of air flow.

Although theoretical and computational investigations of microclimate ensuring systems of clothing are still at the initial stage because of the complexity of phenomena and the inherently multi-scale structure, efforts have been made to explain the main phenomena taking place in the microclimate layer by means of computational modelling. A new finite element structural model has been developed which enables to analyse the air and water vapour mass and heat exchange in multilayer textile packages. Each finite element describes a single layer of the package. Most parameters of the model can be obtained by performing standard measurements. Values of some parameters were adjusted by comparing experimental data with numerical calculations. The model enabled to obtain the temperatures between each pair of textile layers, as well as in the ventilation layer. The time point of sweating could be calculated for any combination of textile materials in the package.

Acknowledgements

This research was funded by a grant (No. MIP-31/2011) from the Research Council of Lithuania.

References

1. Barauskas R, Abraitiene A. Computational analysis of impact of a bullet against the multilayer fabrics in LSDYNA. *International Journal of Impact Engineering* 2007; 34, 7: 1286-1305.
2. Cui Z, Zhang W. Study of the Effect of Material Assembly on the Moisture and Thermal Protective Performance of Firefighter Clothing. *FIBRES & TEXTILES in Eastern Europe* 2009; 17, 6 (77): 80-83.
3. Mattila HR. *Intelligent textiles and clothing*. Published by Woodhead Publishing Limited, Cambridge, England, 2006, p. 506.
4. Korycki R. Method of thickness optimization of textile structures during coupled heat and mass transport. *FIBRES & TEXTILES in Eastern Europe* 2009; 17, 1 (72): 33-38.
5. Bhattacharjee D, Kothari VA. Neural Network System for Prediction of Thermal Resistance of Textile Fabrics. *Textile Research Journal* 2007; 77; 1: 4-12.
6. Sybilska W, Korycki R. Analysis of Coupled Heat and Water Vapour Transfer in Textile Laminates with a Membrane. *FIBRES & TEXTILES in Eastern Europe* 2010; 18, 3 (80): 65-69.
7. Sirvydas PA, Nadzeikienė J, Milašius R, Eičinas J, Kerpauskas P. The Role of the Textile Layer in the Garment Package in Suppressing Transient Heat Exchange Processes. *FIBRES & TEXTILES in Eastern Europe* 2006; 14, 2 (56): 55-58.
8. Li Y, Zhu O. A Model of Heat and Moisture Transfer in Porous Textiles with Phase Change Materials. *Textile Research Journal* 2004; 75, 5: 447-457.
9. Ren YJ, Ruckman JE. Condensation in three-layer waterproof breathable fabrics for Clothing. *International Journal of Clothing Science and Technology* 2004; 16, 3: 335-347.
10. Ghaddar N, Ghali K, Jones B. Modeling of heat and moisture transport by periodic ventilation of thin cotton fibrous media. *International Journal of Heat and Mass Transfer* 2002; 45: 3703–3714.
11. Ghaddar N. et al. Ventilation rates of micro-climate air annulus of the clothing-skin system under periodic motion. *International Journal of Heat and Mass Transfer* 2005; 48: 3151–3166.
12. Ghaddar N, Ghali K, Jones B. Convection and Ventilation in fabric Layers. In: N.Pan, B.Gibson (Eds.) *Thermal and Moisture Transport in Fibrous Materials*. Published by CRC Press, 2006, pp. 271-307.
13. Sun Z, Pan Z. Thermal conduction and moisture diffusion in fibrous materials. In: N. Pan, B. Gibson (Eds.), *Thermal and Moisture Transport in Fibrous Materials*, Published by CRC Press, 2006, pp. 225-270.
14. Bhattacharjee D**,** Kothari VA. Heat transfer through woven textiles. *International Journal of Heat and Mass Transfer* 2008; 44: 375-379.
15. Knitting International, 2002. Breathing Room. Knit Americas. Available at: http://www.inteletex.com/Feature-detail.asp?PubID=27&NewsId=191.
16. Vassiliadis S, Kallivretaki A, Psilla N, Provatidis Ch, Mecit D, Roye A. Numerical Modelling of the Compressional Behaviour of Warp-knitted Spacer Fabrics. *FIBRES & TEXTILES in Eastern Europe* 2009; 17, 5 (76): 56-61.
17. http://www.coolvest.com
18. Bendkowska W, Kłonowska M, Kopias K, Bogdan A. Thermal Manikin Evaluation of PCM Cooling Vests. *FIBRES & TEXTILES in Eastern Europe* 2010; 18, 1 (78): 70-74.
19. Behl M, Lendlein A. Shape-memory polymers. *Materials today* 2007; 10; 4: 20–28.
20. http://www.textileworld.com/Articles/2005/May/Knitting_Apparel/Hydroweave_Protection.html
21. http://www.army.mil
22. http://www.natick.army.mil/soldier
23. Zienkiewitcz OC, Taylor RL. *The Finite Element Method fifth edition.* Published by Butterworth-Heinemann, 2000.
24. Barauskas R., Abraitiene A. Structural Model of Heath and Water Vapor Exchange in Ventilated Multilayer Textile Packages. *Textile Research Journal* 2011; 81, 12: 1195 - 1215.
25. *Textiles. Determination of physiological properties. Measurement of thermal and water-vapour resistance under steady-state conditions (sweating guarded-hotplate test).* LST EN 31092:2002.
26. *Textiles. Determination of the permeability of fabric to air.* LST EN ISO 9237:1997.
27. Mashinskaya GP, Petrov BV. Principles of developing organic-fibre-reinforced plastics for aircraft engineering. In: Shalin, E. R. (Ed.) *Polymer Matrix Composites*, Published by Springer, 1995, pp. 305-422.

Received 02.11.2011 Reviewed 20.04.2012